

Sequential freezing of quadrupolar and dipolar order in (KBr) $_{1-x}$ (KCN) $_x$ Glasses

Alois Loidl, K. Knorr

Angaben zur Veröffentlichung / Publication details:

Loidl, Alois, and K. Knorr. 1986. "Sequential freezing of quadrupolar and dipolar order in (KBr) $_{1-x}$ (KCN) $_x$ Glasses." *Annals of the New York Academy of Sciences* 484 (1): 121–29.
<https://doi.org/10.1111/j.1749-6632.1986.tb49567.x>.

Nutzungsbedingungen / Terms of use:

licgercopyright

Dieses Dokument wird unter folgenden Bedingungen zur Verfügung gestellt: / This document is made available under these conditions:

Deutsches Urheberrecht

Weitere Informationen finden Sie unter: / For more information see:

<https://www.uni-augsburg.de/de/organisation/bibliothek/publizieren-zitieren-archivieren/publiz/>



Sequential Freezing of Quadrupolar and Dipolar Order in $(\text{KBr})_{1-x}(\text{KCN})_x$ Glasses^a

A. LOIDL AND K. KNORR

Institut für Physik

Universität Mainz

D-6500 Mainz, Federal Republic of Germany

The mixed molecular crystals $(\text{KBr})_{1-x}(\text{KCN})_x$ show a fascinating x -versus-temperature phase diagram (FIG. 1).¹ The room temperature structure is of the NaCl type with the CN^- molecules being rotationally disordered. In this plastic high-temperature phase each CN^- ion undergoes fast reorientations. For $x \geq 0.6$ four crystallographic low-temperature phases have been reported^{1,2} where the orientational degrees of freedom are reduced. Only in the orthorhombic phases, for $0.9 \geq x \geq 1$ and $T = 80$ K, is the orientational order complete.² All the other phases exhibit dipolar disorder characterized by a residual degeneracy with respect to head and tail down to the lowest temperatures. Crystals with $x \leq 0.6$ remain in a quadrupolar disordered state of quasi-cubic structure with frozen-in random CN^- orientations and frozen-in lattice strains.^{3,4} As indicated in FIGURE 1, the low-temperature frozen-in state is regarded as a glass state. This can be justified for the following reasons:

1) The freezing is signaled by anomalies in the temperature dependence of the quadrupolar susceptibilities that show striking similarities with the spin glass transition.⁵ In the spin glasses and in the alkali halide-alkali cyanide mixtures frustrated interactions are thought to play the decisive role in the freezing process. In $(\text{KBr})_{1-x}(\text{KCN})_x$ the frustration results from the interplay of site disorder of the CN^- molecules combined with the anisotropic quadrupolar interactions.

2) It has been found that the low-temperature thermodynamic,⁶ ultrasonic,⁷ and dielectric⁸ properties are analogous to those found in canonical glasses and in amorphous solids.⁹⁻¹¹

3) The diffraction data indicate the breakdown of true translational long-range order at the freezing temperature T_F .⁴ This effect is demonstrated in FIGURE 2 by plotting the temperature dependence of the Bragg reflection (440) as measured in a single $(\text{KBr})_{0.5}(\text{KCN})_{0.5}$ crystal.⁴ The data show a well-defined Bragg reflection at 90 K but a strong broadening of the line width as the temperature is lowered. The asymmetry that becomes clearly visible at 10 K can be explained by a bilinear coupling of rotations and translations.³

In studying the relaxation kinetics the reorientational motion of the CN^- ions has been described in terms of dielectric dispersion at frequencies $\nu < 1$ MHz and in terms of elastic dispersion for $\nu > 1$ MHz. Until now the question remained open as to whether both dispersion regimes belonged to the same relaxation mechanism. In this article we will present data on the elastic and dielectric dispersion that cover a common frequency range $10^2 \text{ Hz} \leq \nu \leq 10^9 \text{ Hz}$ and allow a direct comparison of the quadrupolar

^aThis work was supported in part by the Bundesministerium für Forschung und Technologie.

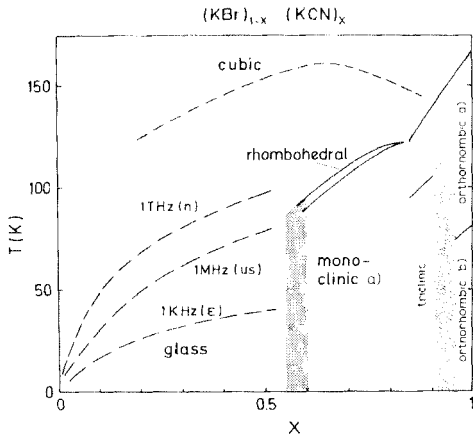


FIGURE 1. Phase diagram of $(\text{KBr})_{1-x}(\text{KCN})_x$.¹ Phase boundaries are shown as solid lines; freezing temperatures, as dashed lines. The hatched area is a coexistence region; the dotted area, the transition region from elastic order to the glass state.

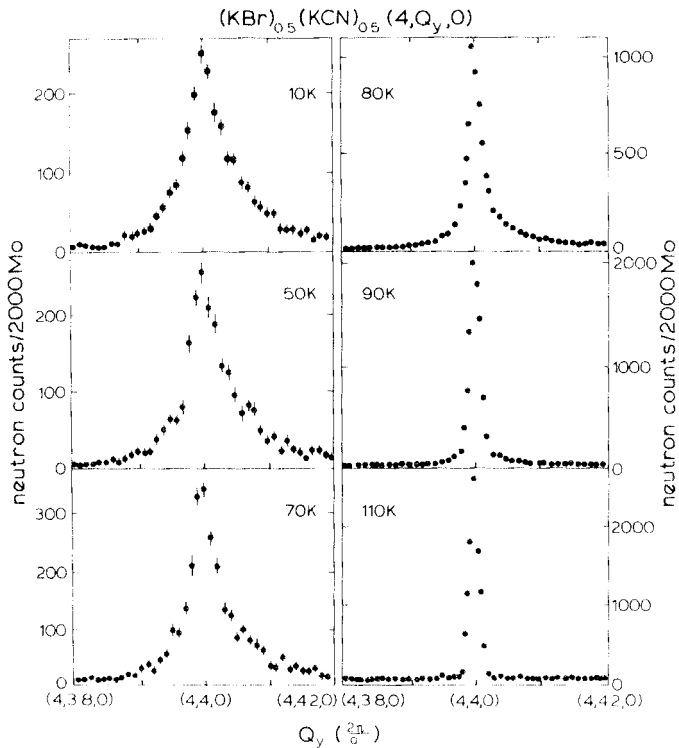
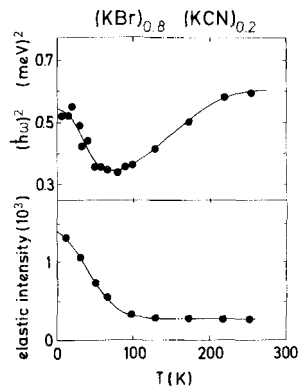


FIGURE 2. Q_y scans at zero energy transfer in $(\text{KBr})_{0.5}(\text{KCN})_{0.5}$ through the reciprocal lattice point (440) at various temperatures.⁴

and the dipolar anomalies. In particular, it will be demonstrated that the freezing-in of dipoles and quadrupoles occurs at different temperatures.

The quadrupolar susceptibility of the orientational subsystem $\chi^Q(T, \nu)$ can be studied via the elastic constant $c_{44}(T, \nu)$ where $c_{44}(T, \nu) = c_{44}^0 \times (1 - g^2 \chi^Q(T, \nu))$. Here c_{44}^0 is the background elastic constant of the center of mass lattice and g^2 is the rotation translation coupling constant. In FIGURE 3 we show the elastic constant $c_{44}(T)$ for $(\text{KBr})_{0.8}(\text{KCN})_{0.2}$ as deduced from the transverse acoustic (TA) phonon dispersion measured at $(2, 0.1, 0)$ TA in an inelastic neutron-scattering experiment.^{12,13} The lower part of FIGURE 3 shows the temperature dependence of the intensity of the central peak as determined at zero energy transfers: c_{44} softens, passes through a minimum, and recovers again towards 0 K. At the minimum sound velocity the central line starts to grow. The central line intensity can be regarded as the order parameter of the glass state.³ The appearance of a central peak immediately demonstrates that the freezing-in of the quadrupolar degrees of freedom is not a single-ion phenomenon but a

FIGURE 3. Squared phonon frequency and elastic intensity at $\mathbf{Q} = (2, 0.1, 0)$ (T_{2g} symmetry) versus temperature, displaying the freezing process in the $x = 0.2$ mixed crystal.



cooperative effect where the strain-mediated interactions between the molecules play an important role.

FIGURE 4 shows the elastic constants and the damping in $(\text{KBr})_{0.965}(\text{KCN})_{0.035}$ as determined from the sound wave propagation along the $[100]$ and $[110]$ directions.¹⁴ The elastic constants, except c_{44} , exhibit a minimum at about 16 K. The attenuation peaks at somewhat lower temperatures. The signal of the c_{44} mode was lost at 22 K because of a large damping, but from the analysis of all the data one can deduce that c_{44} has the same quantitative temperature dependence.¹⁴

The temperature dependence of the elastic constant c_{44} has also been determined by a torsion pendulum with eigenfrequencies ranging from 50 Hz to 1 kHz using capacitive drive and pick-up.¹⁵ The torque is parallel to $[100]$. A representative result for a crystal with the concentration of $x = 0.2$ is shown in FIGURE 5 and compared with the analogous results obtained in the ultrasonic¹⁷ and inelastic neutron-scattering^{12,13} results. In addition Brillouin results for $x = 0.19$ are indicated in FIGURE 5. These results demonstrate the well-known frequency-dependent cusps of the quadrupolar susceptibility.¹⁸

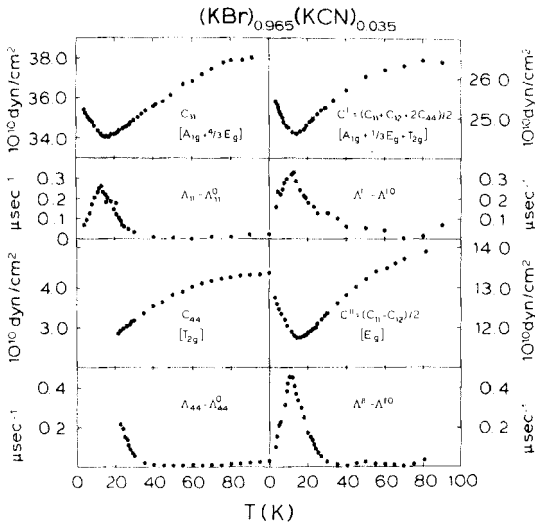


FIGURE 4. The temperature dependence of the elastic constants and the sound-wave attenuation for $(\text{KBr})_{0.965}(\text{KCN})_{0.035}$.¹⁴

Measurements of the dielectric constant $\epsilon(T, \nu)$ probe the dipolar susceptibility $\chi^D(T, \nu)$: $\epsilon(T, \nu) = \epsilon_\infty + 4\pi \times \chi^D(T, \nu)$. The results of the real part of $\epsilon(T, \nu)$ in $(\text{KBr})_{0.8}(\text{KCN})_{0.2}$ are shown in FIGURE 6. The low-frequency data are taken from reference 19. The high-frequency data have been obtained by determining the reflection coefficient and measuring the phase shift utilizing an automatic radio frequency impedance analyzer.¹⁵

Both dipolar and quadrupolar susceptibilities χ^D and χ^Q are given by $\chi^{D,Q}(T, \nu) \propto 1/k_B T / (1 + i\omega\tau^{D,Q}(T))$. Here $\omega = 2\pi\nu$, and τ^D and τ^Q are the dipolar and quadrupolar relaxation times, respectively. As the temperature is lowered the molecular relaxation slows down, yielding dispersion in the real part and a peak loss in the imaginary part of the orientational susceptibility. The maximum in the loss appears at $\omega\tau = 1$, defining the freezing temperatures T_F^Q and T_F^D where the relaxation rates equal a given measuring frequency. A direct comparison between these freezing temperatures can only be performed in the kHz range using dielectric and torsion pendulum data. T_F^Q always appears well above T_F^D . For $x = 0.2$ $T_F^Q = 22$ K and $T_F^D = 17$ K; for $x = 0.5$ $T_F^Q = 63$ K and $T_F^D = 32$ K. Unfortunately, no reliable loss data can be extracted from the ultrasonic and the inelastic neutron-scattering data. Therefore, we took the

FIGURE 5. Normalized elastic constant $c_{44}(T, \nu)$ versus temperature as determined in $(\text{KBr})_{0.8}(\text{KCN})_{0.2}$ for different measuring frequencies: ●: inelastic neutron scattering studies,^{12,13} THz; □: Brillouin data ($x = 0.19$),¹⁶ GHz; +: ultrasonic results,¹⁷ 10 MHz; —: torsion pendulum measurements.¹⁵

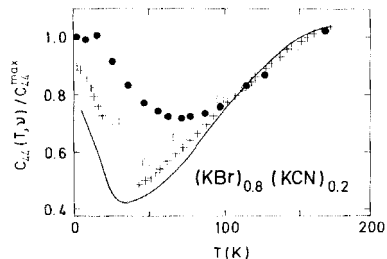
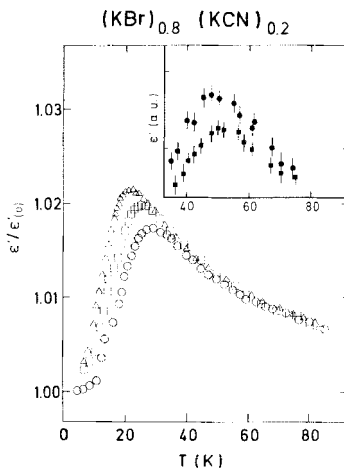


FIGURE 6. Real part of the dielectric constant in $(\text{KBr})_{1-x}(\text{KCN})_x$ versus temperature for different measuring frequencies: \circ : 100 kHz;¹⁹ \square : 10 kHz;¹⁹ \triangle : 87.5 Hz.¹⁹ The high-frequency data are shown in the insert: \bullet : 520 MHz;¹⁵ \blacksquare : 940 MHz.¹⁵



maxima of the real part of the susceptibilities defined by $\min(c_{44}(T, \nu))$ and by $\max(\epsilon(T, \nu))$ as freezing temperatures T_F^Q and T_F^D , respectively. From the dielectric measurements in $(\text{KBr})_{1-x}(\text{KCN})_x$ we know that the maxima of the real part appear 5–10 K above the maxima of the dielectric loss.

FIGURES 5 & 6 reveal that the dispersion regimes for strain and polarization are at different temperatures. For a quantitative comparison we plotted $\ln(\nu)$ versus $1/T_F^Q$ and $1/T_F^D$ for $x = 0.2$ and $x = 0.5$ (FIG. 7). $T_F^D(\nu)$ is well described by an Arrhenius law (solid line) but there exist systematic deviations from Arrhenius-type behavior in the quadrupolar relaxation. The experimentally observed frequency dependence of $T_F^Q(\nu)$ can be described using a phenomenological Vogel–Fulcher ansatz or a power law deduced from dynamic scaling theories.²¹ These descriptions signal a “true” transition into a glass phase. The very limited number of data points, however, hampers a more quantitative analysis.

For both concentrations the freezing temperatures coincide only at GHz frequencies. Significant differences become apparent for lower measuring frequencies. At present, we have no explanation for the dipolar and the quadrupolar freezing

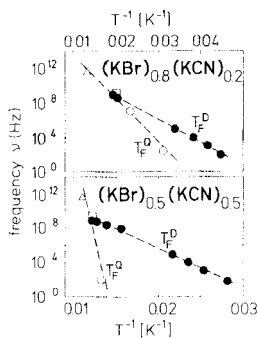


FIGURE 7. Arrhenius plots ($\log \nu$ versus $1/T$) of the dipolar and quadrupolar freezing temperatures in $(\text{KBr})_{1-x}(\text{KCN})_x$ for $x = 0.2$ and $x = 0.5$. Full symbols represent dipolar data.^{15,19} Open symbols represent quadrupolar data: \triangle : inelastic neutron-scattering results for $x = 0.2$ (references 12 and 13) and $x = 0.5$ (references 4 and 20); \square : Brillouin results;¹⁶ \circ : ultrasonic results¹⁷ and torsion pendulum measurements.¹⁵

temperatures becoming identical in the low-GHz range. It is worthwhile to note that GHz frequencies are close to the critical relaxation rate where all the alkali cyanides exhibit a transition for the plastic high-temperature phase into an orientationally ordered state.²² Hence this crossover could define the glass transition temperature T_g . Following arguments by J. M. Rowe (personal communication), the dynamics of the dipoles and the quadrupoles are essentially the same above T_g . At the T_g the onset of spontaneous random strains creates local distortions, thereby increasing the barrier height and introducing an asymmetry into the reorientational potential.²³ Now the quadrupoles spend a longer fraction of time in a preferred orientation yielding a nonzero expectation value of the order parameter of the glass state.³ If this is the case, T_g^Q as determined at THz frequencies is relevant to the paraelastic state, whereas measuring frequencies below 1 GHz probe the glass state.

We have parameterized the quadrupolar and the dipolar susceptibilities in terms of the single-particle-potential Debye-Arrhenius model. The results, namely the hindering barrier E_0 and the attempt frequency $\tilde{\nu}_0$, are shown in FIGURE 8.

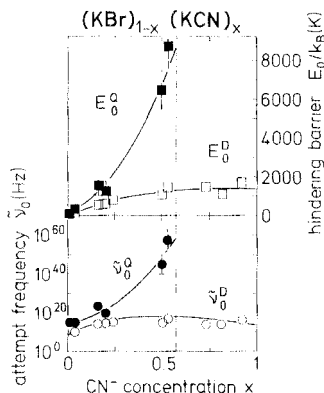


FIGURE 8. Attempt frequencies $\tilde{\nu}_0$ and hindering barriers E_0 versus x as derived from Arrhenius fits to the dipolar and quadrupolar freezing temperatures. Dipolar parameters: \circ : ν_0^D ; \square : E_0^D . Quadrupolar parameters: \bullet : ν_0^Q ; \blacksquare : E_0^Q .

We are aware that an Arrhenius type of analysis of the cusps of the real part of the susceptibilities (and not of the peak maxima of the loss) introduces systematic errors into the parameters E_0 and ν_0 . For the dielectric measurements we performed a rigorous analysis fitting the real and imaginary parts of the dielectric constant within the framework of an Arrhenius model including a symmetric distribution of relaxation times. From this analysis we know that the dielectric parameters as shown in FIGURE 8 are overestimated: the hindering barriers E_0^D are overestimated by a factor of 1.3 to 2; the attempt frequencies ν_0^D , by two to five decades. As stated before, however, no quadrupolar loss data are available at higher frequencies: in the ultrasonic experiments the signals are lost due to heavy damping;^{14,17} in the inelastic neutron-scattering experiments the loss is hidden in the temperature-dependent broadening of the phonon linewidth. An analysis of the neutron data is model dependent and limited by the experimental resolution. Nevertheless, we tried an analysis of the quadrupolar loss data based on neutron and torsion pendulum results in $(\text{KBr})_{0.8}(\text{KCN})_{0.2}$. Again we

found that the hindering barriers and the attempt frequencies as shown in FIGURE 8 are overestimated (E_0^Q approximately by a factor of 1.5, ν_0^Q by five decades). We take this as a proof—although the absolute values of E_0 and ν_0 as shown in FIGURE 8 are systematically too high—that the trends in the quadrupolar and dipolar parameters are well established.

Only at very low concentrations may reasonable values for the quadrupolar parameters be found. With increasing CN^- concentrations E_0^Q and ν_0^Q increase and become unphysically large. It must be clearly stated that a description of relaxational phenomena in terms of Arrhenius-type behavior describes the single-ion case only. Collective effects that we think drive the quadrupolar freezing enter artificially into the free parameters yielding unrealistically high values of $\tilde{\nu}_0$ and E_0 . If one accepts these two parameters as a translation of collective effects into a single-ion picture, one should be aware that $\tilde{\nu}_0$ and E_0 can be rewritten in terms of alternative parameters E and ν_0 where $\nu_0 = \tilde{\nu}_0 \times \exp(-\alpha/k_B)$ and $E = E_0 - \alpha T$. Using this formulation the collective effects are cast more naturally into a linear temperature dependence of the hindering barrier. The parameter ν_0 is a real attempt frequency that could be visualized as the rotation frequency of the free CN^- rotator or as a typical frequency of acoustic shear waves.

The high values and the strong concentration dependence of the quadrupolar single-ion Arrhenius parameters prove that the freezing in $(\text{KBr})_{1-x}(\text{KCN})_x$ is a cooperative phenomenon and that collective effects become more and more important as the concentration is increased. The high values of the hindering barriers demonstrate that the reorientations of a single quadrupole are accompanied by changes in the surrounding strain fields, which trigger the reorientation of neighboring CN^- molecules. The contribution of the single-ion crystalline anisotropy to E_0 is on the order of 50 K and can be neglected when $x \geq 0.1$. A possible interpretation can be given in terms of a cluster formation process: at the glass transition the CN^- ions that are exposed to the strongest random strain fields are blocked in clusters leaving only cooperative relaxation channels for the molecular reorientation. The clusters grow with decreasing temperature and thereby increase the barrier height against molecular relaxation. A distribution of clusters gives the broad distribution of relaxation times that has been observed in $(\text{KBr})_{1-x}(\text{KCN})_x$.²⁴

Conclusions concerning the origin of the dipolar hindering barriers are more difficult to draw. For all concentrations the dipolar freezing is measured in an orientationally ordered or in a quadrupolar glass state. Hence the Arrhenius parameters are relevant to a cubic crystalline potential with local deformations only. FIGURE 8 suggests that the local environment is very similar in the quadrupolar glass and the quadrupolar long-range ordered state. There are no discontinuities at the critical concentration, that is, when $x = 0.6$. Therefore, we agree with Sethna *et al.*²⁵ that the energy barriers to dipolar reorientations depend predominantly on the local deformation of the single-ion potential through quadrupolar interaction forces. At the moment, however, there exist no experimental data that allow us to determine the importance of the dipolar interactions in the dipolar freezing process. These experimental results support the x -versus-temperature phase diagram as proposed by Ihm²⁶ on theoretical grounds.

In conclusion, we have shown that the quadrupolar and the dipolar freezing-in in $(\text{KBr})_{1-x}(\text{KCN})_x$ is decoupled. The quadrupolar freezing is a cooperative phenomenon

whereas the dipolar relaxation is a thermally activated process over the hindering barriers created by the quadrupolar interaction energies.

SUMMARY

Dipolar and quadrupolar susceptibility measurements were reported for the molecular glass system $(\text{KBr})_{1-x}(\text{KCN})_x$ and covered a wide range of frequencies. The results allowed a direct comparison of the dipolar and quadrupolar anomalies and demonstrated unambiguously that the freezing-in of the dipolar and quadrupolar degrees of freedom occurs at different temperatures.

ACKNOWLEDGMENTS

We would like to thank J. M. Rowe for the helpful discussions.

REFERENCES

1. KNORR, K. & A. LOIDL. 1985. *Phys. Rev. B* **31**: 5387.
2. ROWE, J. M., J. J. RUSH & S. SUSMAN. 1983. *Phys. Rev. B* **28**: 3506.
3. MICHEL, K. H. & J. M. ROWE. 1980. *Phys. Rev. B* **22**: 1417.
4. LOIDL, A., M. MÜLLNER, G. F. MCINTYRE, K. KNORR & H. JEX. 1985. *Solid State Commun.* **54**: 367.
5. MYDOSH, J. A. & G. J. NIEUWENHUYNS. 1980. *In Ferromagnetic Materials*. E. P. Wohlfahrt, Ed.: 71–182. Elsevier/North-Holland. Amsterdam.
6. DE YOREO, J. J., M. MEISSNER, R. O. POHL, J. M. ROWE, J. J. RUSH & S. SUSMAN. 1983. *Phys. Rev. Lett.* **51**: 1050.
7. BERRET, J. F., P. DOUSSINEAU, A. LEVELUT, M. MEISSNER & W. SCHÖN. 1985. *Phys. Rev. Lett.* **55**: 2013.
8. MOY, D., J. N. DOBBS & A. C. ANDERSON. 1984. *Phys. Rev. B* **29**: 2160.
9. ANDERSON, P. W., B. I. HALPERIN & C. VARMA. 1972. *Philos. Mag.* **25**: 1.
10. PHILLIPS, W. A. 1972. *J. Low Temp. Phys.* **7**: 351.
11. HUNKLINGER, S. 1977. *In Festkörperprobleme XVII*. J. Treusch, Ed.: 1–11. Vieweg. Dortmund.
12. LOIDL, A., K. KNORR, R. FEILE & J. K. KJEMS. 1983. *Phys. Rev. Lett.* **51**: 1054.
13. LOIDL, A., R. FEILE, K. KNORR & J. K. KJEMS. 1984. *Phys. Rev. B* **29**: 6052.
14. LOIDL, A., R. FEILE & K. KNORR. 1981. *Z. Phys. B* **42**: 143.
15. VOLKMANN, U. G., R. BÖHMER, A. LOIDL, K. KNORR, U. T. HÖCHLI & S. HAUSSÜHL. 1986. *Phys. Rev. Lett.* **56**: 1716.
16. SATIJA, S. K. & C. H. WANG. 1978. *Solid State Commun.* **28**: 617.
17. FEILE, R., A. LOIDL & K. KNORR. 1982. *Phys. Rev. B* **26**: 6875.
18. LOIDL, A., R. FEILE & K. KNORR. 1982. *Phys. Rev. Lett.* **48**: 1263.
19. KNORR, K. & A. LOIDL. 1982. *Z. Phys. B* **46**: 219.
20. ROWE, J. M., J. J. RUSH, D. J. HINKS & S. SUSMAN. 1980. *Phys. Rev. Lett.* **43**: 1158.
21. SOULETIE, J. & J. L. THOLENCE. 1985. *Phys. Rev. B* **32**: 516.
22. LÜTY, F. & J. ORTIZ-LOPEZ. 1983. *Phys. Rev. Lett.* **50**: 1289.
23. STOKES, H. T. & R. D. SWINNEY. 1985. *Phys. Rev. B* **31**: 7133.
24. BIRGE, N. O., Y. H. JEONG, S. R. NAGEL, S. BHATTACHARYA & S. SUSMAN. 1984. *Phys. Rev. B* **30**: 2306.
25. SETHNA, J. P., S. R. NAGEL & T. V. RAMAKRISHNAN. 1984. *Phys. Rev. Lett.* **53**: 2489.
26. IHM, J. 1985. *Phys. Rev. B* **31**: 1674.

DISCUSSION OF THE PAPER

A. NAVROTSKY (*Princeton University, Princeton, NJ*): The model for a range of activation energies rests on the binomial distribution of next-nearest-neighbor occupancies, that is, a random CN-Br distribution. Do experiments detect either clustering (positive ΔH_{mix}) or ordering (negative ΔH_{mix})? If there is local order, how seriously are the theoretical predictions affected? What would be the stable low-temperature structure, as opposed to that in glass? [NOTE: This same question is answered in the discussion of the paper by J. P. Sethna in this volume—*Ed.*]

LOIDL: The momentum transfer dependence Q of diffusive neutron-scattering data were analyzed but no indications of chemical clustering could be detected. Of course, there is a dramatic concentration dependence of the low-temperature structure in KBr:CN. Four stable elastically ordered phases have been detected in a CN⁻ concentration range where $0.6 \leq x \leq 1$. We believe that this polymorphism is essential to understanding the glassy properties: if the crystalline structure of KBr:CN is indifferent to shear distortions, the glass phase can be built by mixing clusters that have different structures.